Use of OpenFOAM® for the Investigation of Mixing Time in Agitated Vessels with Immersed Helical Coils

Alexander Stefan and Heyko Juergen Schultz

Abstract This chapter deals with the investigation of potentials in energy efficiency optimization for widespread agitated vessels. A lab-scale model is derived from an industrially used reactor vessel with immersed helical coils, which is utilized for several chemical basis operations. The model is analyzed with particle image velocimetry (PIV) and laser-induced fluorescence (LIF) concerning velocity and concentration fields, which gives a good validation basis for CFD analysis. However, it is challenging to validate simulations of industrial reactors. In this work, the idea is pursued of comparing the flow fields of simulations and measurements in order to validate the computational results. The simulation task implies the generation of complex geometry meshes, solving for steady-state, as well as for transient solutions, and seeking fast and effective methods. An approach to the validation of technical, large-scale simulation results is proposed through comparison of mixing times in simulations and industrial trial runs.

1 Computational Fluid Dynamics in the Chemical Industry

Fluid dynamics is omnipresent in the chemical industry. Processes of arbitrary complexity involve handling material and energy fluxes. Several works serve as a basis for practical planning and the designing of instruments and apparatuses for production plants. In compliance with given requirements, dimensioning and designing are performed according to pertinent specifications given in standards, monographs, or guidelines. Process simulations are very common in the chemical industry, too. Due to high complexity, simplified and semiempirical models were developed for commonly used apparatuses. Those models are the basis for underlying algorithms in

---

A. Stefan · H. J. Schultz (✉)
Faculty of Chemistry, University of Applied Sciences Niederrhein, Krefeld, Germany
e-mail: heyko_juergen.schultz@hs-niederrhein.de

A. Stefan
e-mail: stalexander@gmx.de

J. M. Nóbrega and H. Jasak (eds.), *OpenFOAM®* ,
https://doi.org/10.1007/978-3-319-60846-4_36

process simulation software. A multitude of software applications serve as an aid for the design and operation of chemical plants.

Computational fluid dynamics simulation tools, however, still occupy a niche in the chemical industry. The big success of CFD in, e.g., aviation or the racing industry is explainable by the fact that it optimizes the final product. In the chemical industry, on the other hand, the optimized object is a tool itself. Due to high implementation effort, as well as the computational and financial costs of commercial CFD, chemical engineers still mostly prefer well-established process simulation tools. As an open and free-to-use CFD tool, OpenFOAM® [1, 2] poses an economic solution and represents huge, previously hidden potential for the optimization of chemical industry utilities, which is demonstrated in this contribution with the example of a stirred process.

1.1 Agitated Vessels in the Chemical Industry

In process engineering, and especially in the chemical industry, agitated vessels are commonly used for a multitude of applications. They have therefore been investigated in numerous papers and monographs [3–14]. Typical basic operations are heating, homogenizing, suspending, blending and chemical reactions. For an appropriate design and the effective operation of agitated vessels, it is necessary to understand the hydrodynamics and the transfer phenomena under the given circumstances. In previous works, good models for different aspects of stirred processes have been given for vessels with and without baffles. It is, however, not possible to formulate a universal model for different design scales of vessels; foremost, not for different equipment and internals. It is therefore necessary to look at each case individually. Experimental investigation quickly reaches its limits concerning applicability and costs. At this point, numerical simulation appears to be of large value. However, the results of numerical calculations have to be validated and verified.

This work follows the idea of developing valid CFD methods and simulation procedures for lab-scale mock-ups, which can be validated using measurement technology. These procedures can then be transferred to the industrial scale for the final optimization task.

2 Heat Exchange in Stirred Vessels

To achieve or maintain a certain temperature in the reactor, it is often necessary to install a heat exchanger inside or on the wall of the vessel. The standard types are diverse types of jacket heating, meander and register pipe, heating plug and helical coil in single or double variant [3]. Thanks to their low complexity and cost, huge exchange area and possibility for simple fixation (on most current baffles at any rate),

Fig. 1 Typical industrial reactor with two immersed helical coils

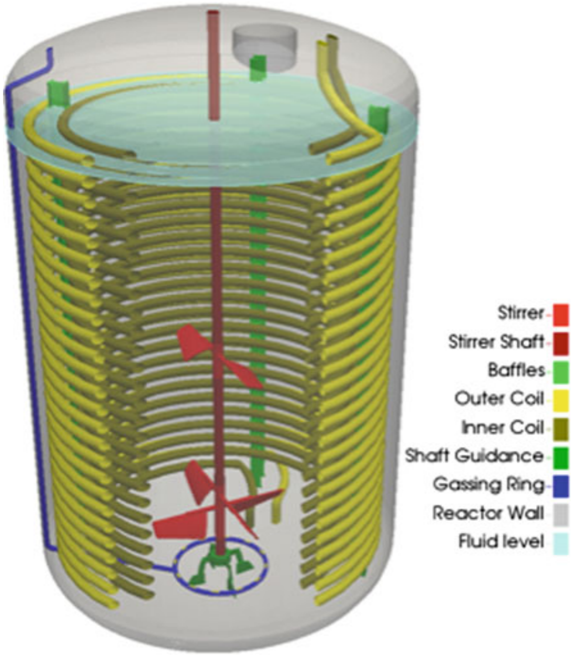

the latter option is very popular in the chemical and biotechnical industries. Figure 1 shows a typical industrial-stirred reactor with double helical coils and four baffles.

The disadvantage of immersed helical coils is the obstacle they pose for fluid dynamics. The works of Bliem and Schultz [15, 16] detail the problems that are caused by coils in regard to velocity fields and heat transfer. Anyhow, a CFD study showed that heat transfer could be improved by up to 24% for the investigated object through optimization of the stirrer position [17].

3 Investigated Object

The simulation study is conducted following the design of the experimental model, which serves as basis for validation. Up to now, little research has been published about vessels with internals, due to the very elaborate measurement approach. For noninvasive optical methods, complex geometries pose a challenging obstacle concerning measurement accuracy. Those problems are caused by image distortion and ray diffraction. This can be circumvented by building the model out of a translucent material. The refractive index of the fluid can then be adapted to it, so that geometries inside the observed domain become invisible and do not disturb the measurement. This method is described in detail in [12]. Bliem investigated the velocity fields via particle image velocimetry (PIV) [16]. The mixing time investi-

Table 1 Surface refinement levels for the snappyHexMesh process

Geometry surface	Reactor wall	Interphase	Stirrer	Baffles	Heater coil	Rigid cylinder
Minimal level	1	1	2	1	2	3
Maximum level	1	1	2	1	2	3

For regions where the surface feature angle is less than 30°, the maximum refinement level is used, otherwise the minimum level

gations were performed by Hirtsiefer via laser-induced fluorescence (LIF) and can be reviewed in [18]. The mixing time was determined by using rhodamine B as the tracer substance. A 10 L beaker glass was used as the vessel, the coil was made out of polymethylmethacrylate (PMMA), and ammonium thiocyanate solution was utilized as the refractive index matched (RIM) liquid. In the scope of this work, high Reynolds numbers between 16,000 and 32,000 were used.

On the simulative side, the described geometry is modeled with the free CAD software Blender® and exported in stl-format. A hexahedral mesh with cells of 5 mm edge length is created with the OpenFOAM® utility blockMesh. It is used for refining and geometry-snapping with the snappyHexMesh utility. A rigid cylinder body is implemented around the stirrer geometry to account for the rotational movement. The local surface refinement levels used in the snappyHexMesh process are listed in Table 1.

Three orthogonal cell layers were added around the heater geometry to suppress numerical diffusion. The same mesh quality controls as in the default implementation of openfoam4 were used for this study. The resulting mesh is presented in Fig. 2.

For simplification, the interphase between gas and liquid is assumed to satisfy slip conditions. This allows for monophasic simulation and is justified by relatively low vortex formation due to the baffles and coil, as, in the scope of the rotating frequencies used, can be demonstrated in experiments and two-phase simulations. Depending on the stirrer used, the final mesh has a size of 1.0–1.4 million cells.

Due to the high Reynolds numbers, a RAS-model (k-epsilon) was used for the simulations.

4 Measurement Approach

4.1 Velocity Field via Particle Image Velocimetry (PIV)

PIV is a rather modern noninvasive optical measurement method for velocity fields. In general, a slice of the flow domain is illuminated via a fanned-out laser beam. Two

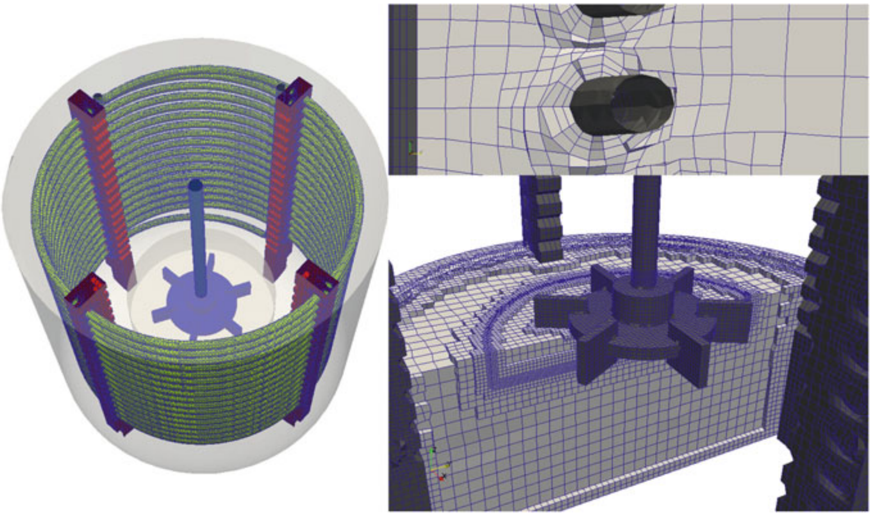

Fig. 2 Details of a snappyHexMesh-generated mesh of a lab-scale reactor with immersed helical coils and a Rushton turbine impeller

images are taken consecutively and the movement of tracer particles is determined by cross-correlation.

The comparison of simulation and measurement data shows good correlation concerning the main flow pattern, as well as transient structures like moving vortices and the fluctuation of the jet stream that is ejected from the stirrer.

The undeniable disadvantage is the limited image area. In standard PIV, only the velocity components inside the plane, but not the so-called out-of-plane component, are detected. This is to be considered when comparing two-dimensional PIV velocity magnitudes with three-dimensional CFD data. The CFD data therefore has to be projected onto the observed plane first. Better results can be achieved with stereo-PIV, in which images are created simultaneously from different perspectives. The out-of-plane component can then be calculated from the angle of the cameras and the differences between the respective images. For more information, see [12].

4.2 Concentration Field via Laser-Induced Fluorescence (LIF)

LIF uses the same experimental setup as PIV. The principle, however, is quite different. A fluorescent substance is used as a tracer. For mixing time investigations, rhodamine B is a good choice, since it is soluble in water and does not noticeably change the viscosity. Thus, its concentration may be considered to be governed by

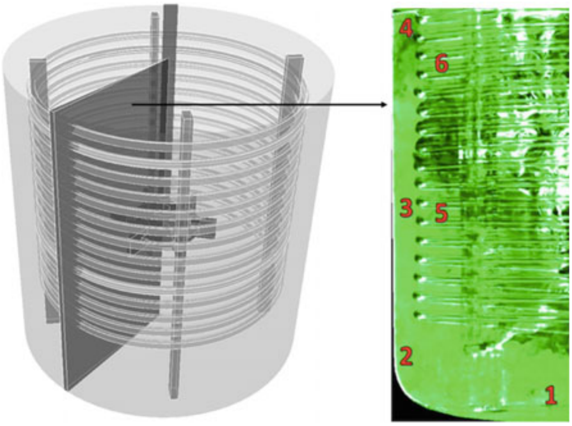

Fig. 3 Probe locations in a vertical slice of a stirred vessel geometry for determination of mixing time via LIF technology

scalar transport. The local intensity of fluorescence can be correlated to the local concentration, which is the basis for determination of mixing time.

Hirtsiefer [18] picked six points in the image for observation of concentration progress. Those points are pictured in Fig. 3.

5 Mixing Time

Mixing time is one of the central feature sizes in a stirred process. It has fundamental influence on both material and thermal transport phenomena. Its value is the basis for process design and the key to determination of the operating parameters and estimation of the energy requirement. However, experimental determination is highly individual for each problem, and even each experimental setup. Nonetheless, it is very important to ensure accurate projection of the experiment to the numerical calculation.

5.1 Definition of Mixing Time

The local concentration $c(x)$ of a tracer substance, where x is the spatial variable, converges to its final concentration c_∞ during the mixing process. The latter can be calculated from the tracer quantity and vessel volume. The current local concentration, however, fluctuates even after reaching a homogenous mixture. It is therefore necessary to specify the relative variance v of the concentration that it is supposed to satisfy the goodness of mixing $M_v = [M_v - v, M_v + v]$. It is common to use a value of $v = 5\%$ [7]. The current local goodness of mixing $M(x, t)$ is defined as the ratio between $c(x, t)$ and c_∞. The mixing time t_m is defined as the point when $M(x, t)$ is inside the interval M_v for all $t > t_\mathrm{m}$ and all x in the domain.

In practice, $c(x, t)$, or any correlated signal, is plotted against time, where $t = 0$ marks the tracer injection time. The final concentration is calculated as a mean value of the signal within a time range in which the mixing time is obviously exceeded. A typical plot is shown in Fig. 5. In this case, numerical data was used. However, the local concentration curves in experiments have similar characteristics. Horizontal margins mark M_v. The signal curve leaves the box for the first time at the mixing time, when viewed from the right side.

5.2 Simulation of Mixing Processes

For investigation of the mixing time, it is necessary to bring the agitated system to a quasi-steady state, in which the main flow field is already developed. In order to augment the efficiency and minimize the calculation cost, a combination of several OpenFOAM® tools is used during the mixing time investigation.

6 Velocity Field

In multiple works, steady-state simulation is used for stirred vessels. It is very fast, and hence a good choice for preliminary studies. A comparison with time-averaged velocity measurement data shows good agreement with this kind of simulation concerning the mean flow pattern [16]. The temporally resolved observation of velocity fields, however, produces evidence of vortex structures that have a comparably long lifetime and move slowly through the flow domain. Those vortices play a crucial role in mixing and must not be ignored. In a steady-state simulation and temporally averaged fields, however, those structures cannot be detected, as they vanish in the mean field. For transient simulations, the OpenFOAM® solver pimpleDyMFoam is used, since it is an adequate solver for large time step, turbulent flows and accounts for the stirrer rotation by dynamic mesh motion.

A steady-state solution is obtained with the simpleFoam solver, including the use of a multi-reference-frame simulation. This is used as an initial condition for transient simulation. After 25 turns of the stirrer, the afore-mentioned vortex structures are developed and the velocity field is assumed to be quasi-stationary. Mixing time investigations can start from these conditions. Snapshots of the resulting vertical velocity fields from CFD and PIV are compared in Fig. 4.

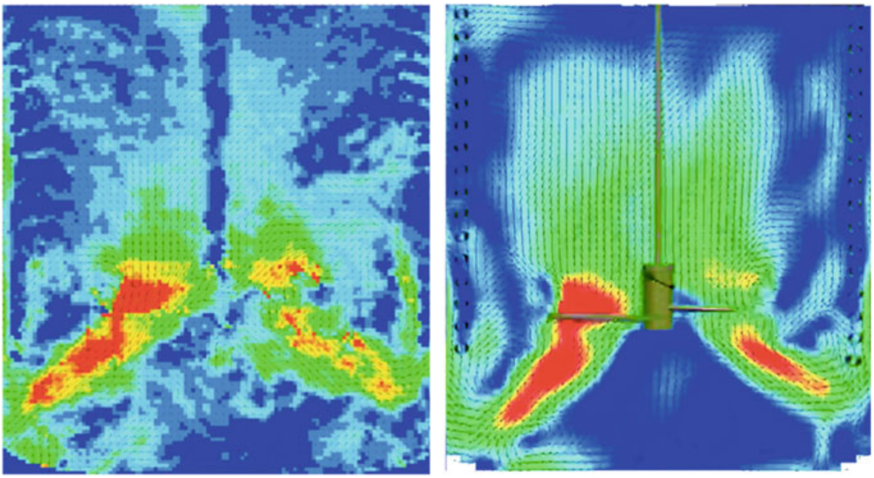

Fig. 4 Comparison of the vertical PIV-measurement (left) and transient CFD (right) results for a pitched blade impeller in a fully turbulent state

7 Tracing via Passive Scalar Transport on Existing Velocity Fields

A passive scalar transport equation is easy to implement on an existing solver in OpenFOAM®, as has been described in numerous tutorials on the web [19] or in [20].

If the mixing time is to be investigated under novel geometry or operating conditions, it is sensible to use the afore-mentioned quasi-stationary field as an initial condition and use the pimpleDyMFoam, extended by the scalar transport equation

$$\frac{\partial}{\partial t}\psi = \nabla \cdot (\Gamma \nabla \psi) - \nabla \cdot (\boldsymbol{u}\psi),$$

where ψ is the scalar of interest, $\boldsymbol{u}$ the velocity, and Γ the scalar diffusion coefficient.

If, however, velocity fields are present from other work, they can be reused for calculation of the mixing time. This method spares one the extremely time-consuming transient calculation of the velocity and pressure fields. The present velocity data indeed have to be adequately temporally resolved and have to reach over a time range that safely exceeds the mixing time. This approach is also especially useful when mixing times with different tracer injection spots, but the same velocity fields, have to be compared. In this case, only the scalar transport has to be calculated twice.

Mimicking the experimental trial, in the simulation, the tracer injection is implemented by setting ψ to the value 1 (setFields utility) on a domain that corresponds to the tracer volume and injection spot, while the residual ψ field remains at 0. Since the tracer is injected quickly in experiments, the domain has the shape of a column. Two injection spots, centric and eccentric, are selected and compared.

8 Determination of Mixing Time at Probe Locations

The measurements of local concentrations during the mixing process were taken at six different points in the vessel (see Fig. 5). The OpenFOAM® utility “probeLocations” allows for analogous tracking of local tracer concentrations. For each of these locations, the local mixing time is determined in the manner described above. Of course, the local mixing times can differ due to dead zones. The total mixing time is assumed to be reached with the latest local mixing time. The exactness of such a method is questionable since local mixture goodness cannot be ensured throughout the entire domain. Possible dead zones, which extend the mixing time, may not be detected. Due to limitations in measurements, the available data are very sparse, and hence the described method is usually practiced.

9 Determination of Global Mixing Time

In CFD simulations, field data for the total volume of the domain are available. Local mixture goodness can be tracked at each computational cell. Following the 95% criterion, all cells that have a concentration higher than the lower margin of $M_{0.05}$ are extracted. The point that marks the mixing time is when the integral of these extracted cells reaches the total domain volume. This method is comparable to the first

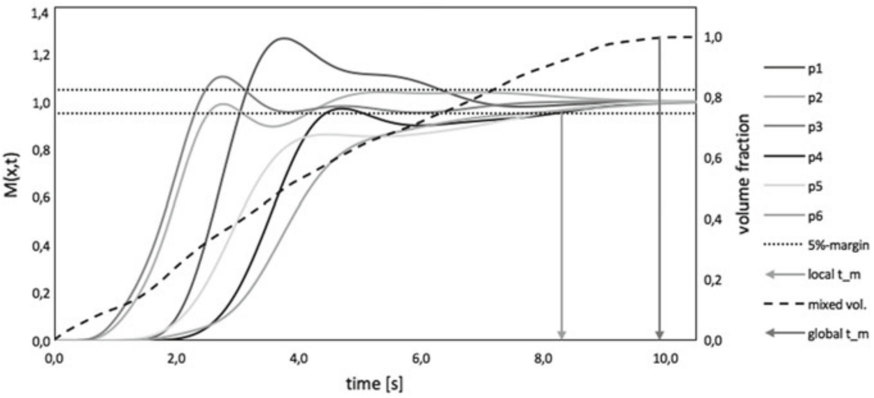

Fig. 5 Mixing time determination in a baffled vessel with a coil and Rushton stirrer at 200 rpm and a central tracing spot. Local and global determination strategies lead to different mixing time values

presented procedure if the probe locations cover the whole domain representatively. With a rising number of probes, the mixing time determined by the first method converges to the global mixing time. Both described methods are compared in Fig. 5. In the present case, the mixing time determined at six probe locations (see Fig. 3) is 8.3 s, but it is 9.8 s when determined globally.

10 Time Resolution for Scalar Transport

For the transient solution of velocity data, the Courant number Co [21] plays an essential role in regarding the time step size. It gives a good control mechanism for adaptive time discretization and is often indispensable for numerical stability. In the case of passive scalar transport, the time step has no influence on the stability, since only the actual velocity field is used in the equation. Rather, it is far more important that the temporal consistency, as it is defined in [21], be ensured, i.e., with decreasing step size, the results must converge to the analytical solution of the equation. An exemplary case would be a time resolution of $T/6$, where T denotes the stirrer revolution time, according to the finest resolution of $Co = 2$ to the stage of 95%. This is an acceptable compromise between accuracy and the additional amount of velocity and mesh data needed for further time resolution.

11 Validation of CFD Results

The CFD results for mixing time are validated with measurement data from [18]. For this study, different stirrer types, rotational frequencies and injection spots were chosen. The simulation and measurement results are plotted in Fig. 6. The results have linear dependency, although the measured mixing times are proportionally higher by a factor of 3. The reason for this discrepancy may be based on the simplicity of the simulation. The tracer concentration is simulated by a scalar transport equation, which does not account for possible interaction with or influence on the transport properties of the fluid. Further reasons can be based on certainty issues of the experimental work. The referenced work of Hirtsiefer [18] points out these problems. However, a correlation between CFD and LIF results is obvious.

12 Conclusions and Outlook

The meaning of CFD is still being underestimated in the chemical industry. The work contributed in this chapter is a demonstration of industrial application possibilities of the example of mixing time determination in an agitated vessel. Several OpenFOAM$^{®}$ and other free software utilities are used in the workflow. Transient quasi-stationary

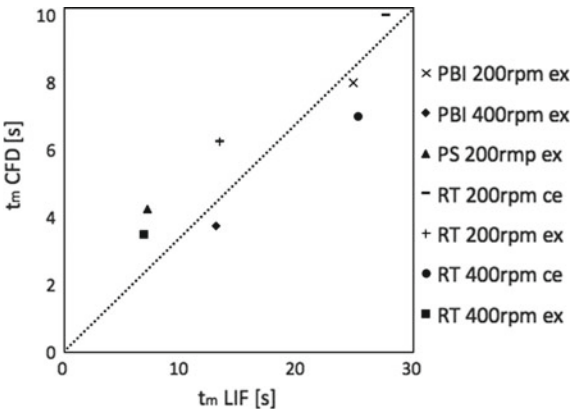

Fig. 6 Comparison of CFD and LIF results. Three different stirrer types are used: PBI—pitched blade impeller; PS—paddle stirrer; RT—Rushton turbine. Two rotational frequencies and two injection spots are chosen: centric and eccentric

velocity fields are used as initial conditions for a concentration-based mixing time determination method. The concentration is mimicked by the implementation of a positive scalar field, which is bounded to 1 at the highest concentration. A memory and computational time-saving method is used for this investigation. The CFD results coincide with LIF data proportionally, although the mixing time is predicted as three times lower than measured. This endorses the principals of the presented procedure and is valid for optimization research, since it reflects the tendencies very well, even under variation of independent parameters.

These results encourage application of the presented methods to industrial scale apparatuses for energy and product optimization, even beyond mixing time investigations. Recently, optimization of energy efficiency has attracted huge interest in industry. In the search for suitable instruments for its realization, CFD has the capacity to play a central role. In this context, OpenFOAM® poses a powerful and economical solution.

Acknowledgements The authors thank all those involved in the organization of OFW11 and all the contributors who have enriched this event. This project upon which this chapter is based is funded by the Federal Ministry of Education and Research under the project number: 03FH020PX4. Responsibility for the contents of this publication rests with the authors.

References

1. OpenCFD Ltd (2004–2016) OpenFOAM®. http://openfoam.com. Accessed 30 Sep 2016
2. Jasak H (2009), OpenFOAM®: Open source CFD in research and industry. Inter J Nav Archit Oc Engng 1:89–94. https://doi.org/10.2478/ijnaoe-2013-0011
3. Zlokarnik M (1999), Ruehrtechnik: Theorie und Praxis. Springer, Berlin Heidelberg
4. Kraume M (2003), Mischen und Ruehren. WILEY-VCH Weinheim
5. Ekato Holding GmbH (2012), Ekato. The Book. Ekato, Freiburg
6. Oldshue JY (1983), Fluid Mixing Technology. Chemical engineering McGraw-Hill Pub. Co., New York

7. Paul EL, Atiemo-Obeng VA, Kresta SM (eds) (2004), Handbook of Industrial Mixing. WILEY-INTERSCIENCE, Hoboken, New Jersey
8. Paschedag AR (2004), CFD in der Verfahrenstechnik. WILEY-VCH, Weinheim
9. Tatterson GB (2003), Fluid mixing and gas dispersion in agitated tanks. Gary Tatterson
10. Lohse R (2008), Simplified Calculation of Mixing and Suspending Processes in Agitated Vessels, Chem. Eng. Technol. 31(12):1799–1805
11. Platzer B (1988), Modeling of the Local Destributions of Velocity Components and Turbulence Parameters in Agitated Vessels – Method and Results. Chem. Eng. Process 23:13–31
12. Jaehrling K, Wolinski S, Ulbricht M, Schultz HJ (2016), Vergleich von Tubebaffles und Rohrschlangen in Bezug auf thermische und mechanische Energieeintragung in Ruehrreaktoren. Chem. Ing. Tech. 88(9):1224. https://doi.org/10.1002/cite.201650211
13. Stefan A, Wuenscher P, Schultz HJ, Ulbricht M (2016), Untersuchung der Gasdichteverteilung in begasten Ruehrkesseln mit eintauchenden Rohrschlangen. Chem. Ing. Tech. 88(9):1385–1386. https://doi.org/10.1002/cite.201650341
14. Schultz HJ, Matzke M, Kessel C, Jaehrling K, Stefan A, Bliem V (2016), Experimente und gekoppelte CFD-Simulationen von Wärmeübergängen an Rohrschlangen in Fermentern und Rührreaktoren. Chem. Ing. Tech. 88(9):1380. https://doi.org/10.1002/cite.201650216
15. Bliem V, Schultz HJ (2014), Investigation of Horizontal Velocity Fields in Stirred Vessels with Helical Coils by PIV. International Journal of Chemical Engineering. https://doi.org/10.1155/2014/763473
16. Bliem V (2016), Untersuchung des Einflusses der Stroemungsverhaeltnisse auf den Waermeuebergang in Ruehrreaktoren mit Rohrschlangeneinbauten mittels PIV/LIF. Dissertation, University of Duisburg-Essen
17. Stefan A, Hindges S, Schultz HJ (2016), Simulation of the Heat Exchange in Vessels with Helical Coils and the Influence of Stirrer Position. Chem. Ing. Tech. 89(4):470-474. https://doi.org/10.1002/cite.201600146
18. Hirtsiefer M (2015), Investigation of Heat Transfer and Mixing Characteristics of Helical Coils in Stirred Tank Reactors by Laser-induced Fluorescence. Master Thesis, University of Applied Sciences Niederrhein
19. 11th OpenFOAM® Workshop (2016) Training Courses. openfoamworkshop.com. Accessed 30 Sep 2016
20. Maric T, Hoepken J, Mooney K (2014), The OpenFOAM® Technology Primer. Sourceflux
21. Ferzinger JH, Peric M (2002), Computational Methods for Fluid Dynamics. Springer, Berlin Heidelberg